

Multi Classification of Alzheimer's Disease using Linear Fusion with TOP-MRI Images and Clinical Indicators

Qiao Pan, Golddy Indra Kumara, Jiahuan Chu
School of Computer Science
Donghua University, Shanghai, China
panqiao@dhu.edu.cn, gikumara@outlook.com, 1944362@qq.com

Abstract—With the development of artificial intelligence, computer-aided diagnosis plays an increasingly important role in Alzheimer's disease (AD). In this paper, a new multi-classification diagnostic algorithm based on TOP-MRI images and clinical indicators is proposed. The features of TOP-MRI images and clinical indicators are fully exploited for multi-classification diagnosis of AD. First, we design TOP-CNN-NN model based on three VGGNet-16 convolutional neural networks and a single hidden layer neural network to extract the image feature vector of brain three orthogonal planes (TOP) MRI images. Then we screen clinical data using CfsSubsetEval evaluator to compose clinical feature vector. Then, the image feature vector and indicator feature vector are fused by using linear fusion method of multi-source data based on canonical correlation analysis (CCA). Finally, the fusion vector becomes the input for multi-classification classifier to distinguish three stages of AD: control normal (CN), mild cognitive impairment (MCI) and Alzheimer's disease (AD). The proposed algorithm is validated using the Alzheimer's Disease Neuroimaging Initiative (ADNI) dataset. Experiments show a good performance since the accuracy of the proposed algorithm in the multi-classification of AD can reach 86.7%.

Keywords— Alzheimer's disease; linear fusion; multi-source data; multi-classification; deep learning

I. INTRODUCTION

Alzheimer's Disease (AD) is a neurodegenerative disease characterized by progressive cognitive decline that irreversibly affects all cognitive functions of human brain, and ultimately leads to severe impairment or premature death of the individual's daily activities [1]. According to [2], 50 million people are suffering from AD in 2018. About 8% of the elderly aged 65 to 85, and 35% aged 85 and over are affected by AD disease [3]. Clinically, AD is divided into three stages: control normal (CN), mild cognitive impairment (MCI), and Alzheimer's disease (AD). MCI is the early manifestation of AD, the transition state from CN to AD [4].

Magnetic resonance imaging (MRI) is often used as a basis for diagnosing AD due to its spatial resolution, high accessibility, and good contrast [6]. Common methods for computer-aided diagnosis of AD using MRI images are extracting features based on 3D medical images, using region of interest (ROI) to diagnose AD, and using image segmentation to measure the morphology of hippocampus, entorhinal cortex and amygdala to diagnose AD [8].

However, there are still problems in these methods including difficulty in designing algorithms based on 3D medical images due to their high dimensionality, noise and sparsity.

This paper proposes a new multi-classification diagnostic algorithm based on TOP-MRI images and clinical indicators. The three orthogonal planes (TOP) is a tangent plane in three directions centered on the spatial geometric center of the brain, clinical indicators include demographic information, neuropsychological assessment and biological detection. The main contributions of this paper are as follows:

- There is no need to label and divide ROI in extracting image feature vector by using TOP-CNN-NN model, which reduces the difficulty of prior knowledge.
- Only three different planar MRI images are needed to mine brain feature information. It avoids the difficulty of representation and modeling, which also improves the efficiency of model training and classification.
- CCA is used to fuse TOP-MRI image feature vector and clinical indicator feature vector. Considering various types of data, it conforms to the clinical reality. The validity of the proposed classification model is verified by using ADNI data sets.

II. RELATED WORK

Nowadays most methods of AD classification diagnostic study is to pre-process MRI image, extract features from the image and input the features into the classifier to predict diseases. AD multi-classification is proposed by Hiroki Karasawa using deep convolutional 3D neural network made of 36 Convolutional Layers 1 Dropout Layer, 1 Average Pooling Layer and 1 FC Layer in general [9]. Carlos Platero et al. raised a Hippocampal segmentation based on patch method and non-rigid registration label fusion method. ROI was marked initially by means of non-rigid registration label fusion method first, and then marked by means of patch method [10]. Devvi Sarwinda used oriented gradients of three orthogonal planes histogram to extract dynamic texture features, then they took advantage of probability principal component analysis (PPCA) for dimensionality reduction, and sort AD, MC, NC using random forest classifier [7]. Tooba Altaf et al. present a classification method of combined features, adopting MRI image textural feature

method with clinical data. In image textural feature extraction, segmenting the image into three areas: gray matter, white matter and cerebrospinal fluid, extracting features by means of GLCM, SIFT, HOG and LBP techniques, gaining clinical data by adopting characteristic indexes of FAQ, NPI, GDS [11]. Tong T. et al. present a nonlinear graph fusion (NGF) method to gain the complementary information across modalities [12].

III. METHODS

The multi-classification diagnosis algorithm proposed includes four modules: image feature extraction, indicator feature selection, feature vector fusion and disease classification diagnosis. Fig. 1 shows the framework of the algorithm.

In the image feature extraction module, three MRI images from the three orthogonal planes of the brain are selected. The images are pre-processed and then input them into the TOP-CNN-NN model to extract image feature vector. In the indicator feature selection module, the clinical indicators are selected by CfsSubsetEval evaluator and combined to form indicator feature vector. In the feature vector fusion module, image feature vector and indicator feature vector are linearly fused by Canonical Correlation Analysis (CCA). In the disease classification diagnosis module, input the fusion feature vectors to the multi-classifier to distinguish the three stages of AD: control normal (CN), mild cognitive impairment (MCI), and Alzheimer's disease (AD).

A. Image feature extraction

In this module, TOP-CNN-NN model is constructed to extract the feature vector from the MRI images. The model consists of three VGGNet-16 convolutional neural networks (CNN) and a single hidden layer network (NN). The framework is shown in Fig. 2.

First, The MRI image is pre-processed, then it is extracted to the VGGNet-16 convolutional neural network. Second, the three preliminary feature vectors from the VGGNet-16 are weighted by voting. Lastly, input the weight vector into the

single hidden layer network to generate the fusion feature vector.

1) Image pre-processing

In this module, three orthogonal planes (TOP) MRI images are selected as input of image feature extraction model. TOP MRI images contains important information for the diagnosis of AD, such as the hippocampus, entorhinal cortex and amygdala.

Different planar images show that patients with AD have atrophy, ventricular enlargement and other pathological features compared with normal (CN) and mild cognitive impairment (MCI) patients, as shown in Fig. 3.

Many problems on MRI images occurs from the detection equipment and techniques such as irregularity, high noise, different shade, etc. To solve these problems, this module uses three steps to pre-process the image. The steps are as follows:

a) Geometry transformation

The main purpose of geometry transformation is to improve the spatial position of brain imaging area in MRI images. It is used to correct the systematic errors of magnetic resonance imaging (MRI) instruments and the random errors of imaging position (e.g. imaging angle, perspective relationship). In this module, translation and rotation are used to solve the problems of image position offset and angle deflection caused by imaging angle in brain MRI images. Zoom is used to unify different size of brain images caused by the difference of perspective relationship.

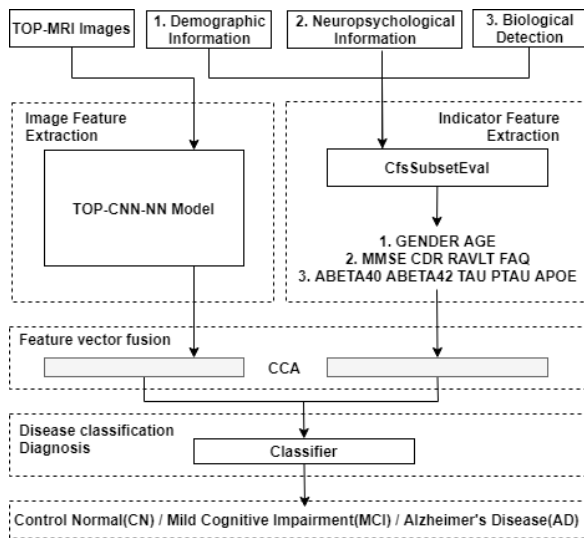


Fig. 1. Framework of Multi-Classification Diagnosis Algorithm

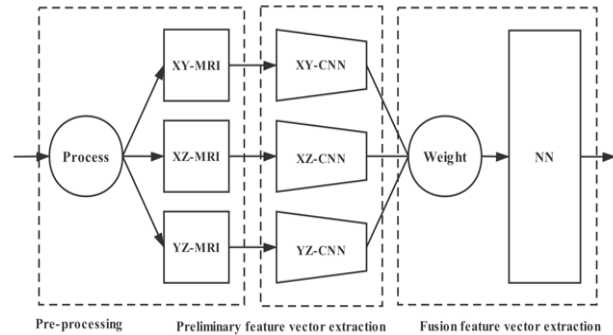


Fig. 2. TOP-CNN-NN image feature extraction model framework

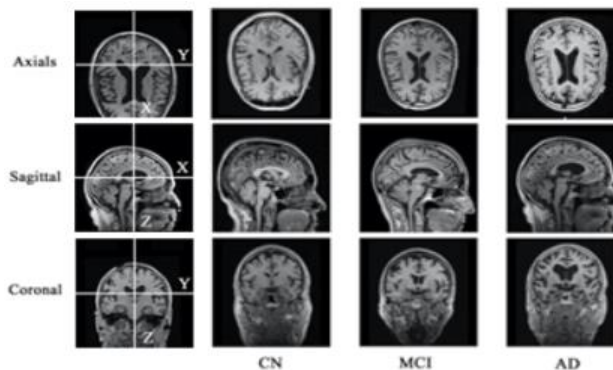


Fig. 3. Different brain planes of patients' MRI images with CN, MCI, AD

b) Image noise reduction

In this module, salt-and-pepper noise is processed by median filter, and Gaussian noise is processed by Gaussian filter. The median filtering technology makes the image smooth by sorting the pixels in the field according to the gray level, and then choosing the median value in the group as the output pixel value. Gaussian filtering is a weighted averaging process for the whole image. The value of each pixel is obtained by weighted averaging of its own and other pixel values in its neighborhood. The coordinates with domain size of $(2n+1) \times (2n+1)$ are brought into (1) to calculate the pixel values of the corresponding coordinates:

$$G(x, y) = \frac{1}{2\pi\sigma^2} e^{-\frac{(x-n-1)^2 + (y-n-1)^2}{2\sigma^2}} \quad (1)$$

where x, y is the coordinates of the pixels, σ are the values that need to be set.

c) Standardization

The purpose of pixel value standardization is to scale the original image pixel value and limit the pixel value to a certain range. The standardization process is defined as:

$$MRI_s = \frac{MRI - \mu}{\max(\sigma, \frac{1.0}{\sqrt{N}})} \quad (2)$$

where MRI is the image matrix, μ is the image mean, σ is the standard variance, and N is the number of MRI image pixels. Consistent input data can be obtained by standardization, which will avoid different shades and contrast problems. It can improve the convergence speed of the model and the accuracy of the classification diagnosis model.

2) Preliminary feature extraction

Convolutional Neural Networks (CNN) is a class of feedforward neural networks with convolutional computation and deep structure, which has been widely used in image fields [13]. In this module, we use VGGNet-16 to obtain the tangential images of the three orthogonal planes of the brain: Axials, Sagittal, and Coronal. Then these three tangential images are trained for XY-CNN, XZ-CNN and YZ-CNN. These three CNN models are used to extract the preliminary feature vector of the respective planes.

VGGNet is a deep convolutional neural network that explores the relationship between the depth of the convolutional neural network and its performance. By repeatedly stacking 3×3 small convolution kernels and 2×2 maximum pooling layers, a convolutional neural network has been constructed with 16-19 layers. In this module, the model is based on VGGNet-16, which is shown in Fig. 4.

The input of VGGNet-16 is RGB image of 224×224 size. In the process of image convolution, the feature map MRI_i representing layer i of VGGNet-16 is used. Assuming that



Fig. 4. Network parameters of VGGNet-16 model

MRI_i is a characteristic graph of convolution layer, its generating process can be described as:

$$MRI_i = f(MRI_{i-1} \times W_i + b_i) \quad (3)$$

where W_i is the weight vector of the i^{th} layer convolution kernel. The operation symbol " \times " is the convolution operation of the convolution kernel and the $(i-1)^{\text{th}}$ layer image or feature map, and the output of the convolution and the offset vector of the i^{th} layer b_i are added. The feature map MRI_i of the i^{th} layer is obtained by the nonlinear excitation function $f(x)$. The VGGNet-16 model uses a 23-layer convolution layer. The low-level convolutional layer of the model extracts some low-level features such as edges and lines. The high-level convolutional layer of the model iteratively extracts more complex features from low-level features. After each convolution layer, a max pooling layer is added for more complete and important features. Assuming that MRI_i is the Max pooling layer, its generating process can be defined as:

$$MRI_i = \text{Maxpooling}(MRI_{i-1}) \quad (4)$$

For several image feature values extracted by filter, max pooling only retains the largest pooling layer feature. This operation can reduce the number of model parameters and reduce the over-fitting problem. Finally, VGGNet-16 uses the 3 fully connected layer to combine the extracted features. Assuming that full connection layer has p parameters, x_n is the input or n feature graphs, and its generating process can be defined as:

$$FC_p = W_{p1} * x_1 + W_{p2} * x_2 + \dots + W_{pj} * x_n + b_p \quad (5)$$

where p is the number of the full connection layer and w is the weight matrix. Each neuron in the connective layer is fully connected to all the neurons in the preceding layer. Full connection layer can integrate local information with category discrimination in convolution layer. The initial eigenvector mentioned in this chapter is the output of the last full connection layer in VGGNet-16. The dimension of preliminary feature is 1000.

3) Fusion feature vector extraction

Since each planar image in three orthogonal planes (TOP) of the brain has its own characteristics, there are differences in the regions and expressions of interest in the VGGNet-16 feature extraction process. A voting weighted vector fusion method as shown in Fig. 5 is adopted, which can highlight the respective features and reduce the vector fusion problem caused by feature differences.

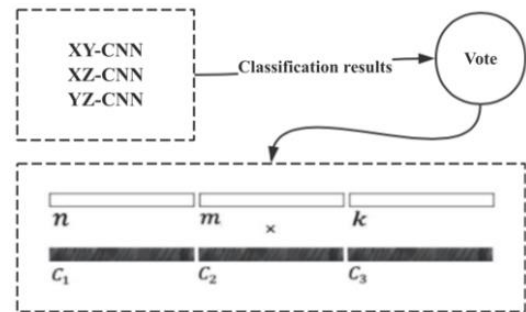


Fig. 5. Voting weighting process of image preliminary feature vector

Firstly, by counting the classification results corresponding to the TOP. If the classification results are the same, use it as the voting result, otherwise the higher classification accuracy will be taken as voting result. Then, each voting result corresponds to a weight vector. Assume that the preliminary feature vectors of XY-CNN, XZ-CNN, and YZ-CNN are $C_1=\{\alpha_1, \dots, \alpha_{1000}\}$, $C_2=\{\beta_1, \dots, \beta_{1000}\}$ and $C_3=\{\gamma_1, \dots, \gamma_{1000}\}$, respectively. Then the voting weighting operation can be defined as:

$$C = (n\alpha_1, \dots, n\alpha_{1000}, m\beta_1, \dots, m\beta_{1000}, k\gamma_1, \dots, k\gamma_{1000}) \quad (6)$$

where n, m and k are weighting factors. After changing the values of the weighting factors n, m and k, the proportions of the three preliminary feature vectors in the fused feature vector are no longer balanced. In the process of setting the weighting factor, assuming that the classification result of one of the planes is the same as the voting result, the preliminary feature vector weight extracted by the plane is increased.

Finally, input the voting weighted feature vector C into the single hidden layer neural network. The single hidden layer neural network will fuse the feature vector of three orthogonal planes and output the fusion feature vector with lower dimension, which is beneficial for the linear fusion on the next step with the clinical indicator feature vector, and avoid the over-fitting problem. The image feature vector output by the TOP-CNN-NN model is the hidden layer output of the single hidden layer network, and the dimension of the fusion feature vector is 50.

B. Indicator feature selection

The ADNI dataset contains clinical information for each subject, such as gene detection, demographic information, neuropsychological assessment, biological detection, etc.

In this module, we use the CfsSubsetEval evaluator to evaluate the classification capabilities and redundancy of each indicator. During the evaluator's selection, the indicators with high correlations with disease classification results but low correlations with each other are selected. As long as the subset does not contain indicators that are more relevant to the current indicator, the indicators that are most relevant to the disease classification results are continuously added. The evaluator will use the missing value as a separate value, or it can distribute the missing value count along with the other values according to the frequency of occurrence. Selecting a subset of indicators can also help eliminating irrelevant and duplicate indicators. The relationship between the two indicators I_1 and I_2 can be measured by symmetric uncertainty, defined as:

$$U(I_1, I_2) = 2 \frac{H(I_1) + H(I_2) - H(I_1, I_2)}{H(I_1) + H(I_2)} \quad (7)$$

where the basis of the entropy function H is the probability of each indicator. $H(I_1, I_2)$ is the joint entropy of I_1 and I_2 , it is calculated from the probability of all combinations of I_1 and I_2 . The range of uncertainty is 0-1.

Feature selection based on correlation determines the superiority of an indicator set, defined as:

$$R = \frac{\sum_j U(I_j, C)}{\sum_i \sum_j U(I_i, I_j)} \quad (8)$$

where C is the category of AD, and I_i and I_j are all indicators in the indicator set.

Through the CFS evaluator, this module selects 11 indicators as clinical indicators. There are 3 types of clinical indicators: demographic information, neuropsychological assessment, and biological detection. Demographic information consists of patients' gender and age.

The indicators for neuropsychological assessment are Mini-Mental State Examination (MMSE), Clinical Dementia Rating (CDR), Rey Auditory Verbal Learning Test (RAVLT), and Functional Activity Questionnaire (FAQ). MMSE is the most common scale for clinically examining intelligence. It can comprehensively, accurately and quickly respond to the mental state and the degree of cognitive impairment of the subject. The patient's condition is reflected by the total score of the scale.

The CDR is obtained by retrieving information from patients and their families to complete the cognitive impairment degree assessment, which will quickly assess the severity of the patient's condition. Areas of assessment include memory, orientation, judgment and problem-solving skills, work and social skills, family life and personal hobbies, and the ability to live independently.

The RAVLT immediate and delayed test evaluates the patient's speech memory. The patients will listen to a certain amount of content in this test and then performs immediate and delayed recall to judge their condition. Studies have shown that RAVLT distinguishes AD from other neuropsychological assessments [14]. Lastly, the details regarding daily chores is measured in FAQ. Activities that require higher cognitive abilities can prove to be quite useful in assessing the condition of dementia subjects.

The indicators for biological detection are amyloid β -peptide ($A\beta$), Tau protein (Tau), water-soluble phosphorylated Tau protein (P-Tau), and Apolipoprotein E (ApoE 4). Amyloid β is the main component of senile plaque, which is a characteristic of neuropathology of AD. The most important $A\beta$ are $A\beta_{40}$ and $A\beta_{42}$ [14]. The study found that the amyloid beta protein in brain tissue of AD patients increased significantly [17], therefore the detection of plasma $A\beta$ levels is helpful for detecting AD.

Tau protein is a microtubule-related protein with low molecular mass, and is prone to form paired helical filaments (PHFs) after abnormal phosphorylation and glycosylation, and further constitute neurofibrillary tangles, which are the characteristic pathological manifestations of AD [14]. The level of tau protein in the cerebrospinal fluid of patients with moderate to severe AD was significantly higher than the normal CN subjects, and the increase of this index was earlier than the occurrence of clinical dementia symptoms, which can be used for the prediction of AD [15].

ApoE is one of the most important apolipoproteins in the central nervous system. It is involved in the mobilization and redistribution of cholesterol. It is also necessary to maintain

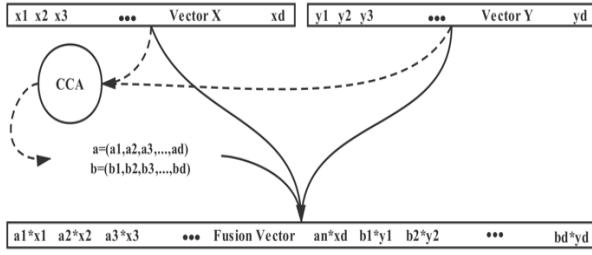


Fig. 6. Feature vector fusion process based on CCA

the integrity of myelin sheath and neuron cell membrane after the development and injury of the nervous system [14], and its protein level in plasma is affected by ApoE genotype. Related studies have shown that patients with ApoE genotype have a higher risk of progression from MCI to AD, thus ApoE has a certain reference for the diagnosis of AD [16].

C. Feature vector fusion

Multi-source data fusion integrates data from different data types through some data fusion rules, absorbs the characteristics of different types of data, and extracts standards from them. It is better and has more rich information than single data.

Multi-source data can be fused at three levels: vector level, feature level, and decision level. Decision-level fusion is achieved by synthesizing the classification results of multiple classifiers. However, decision-level integration is not suitable for the fusion of images and indicators; Feature-level fusion is a more common way, and descriptive that can express the correlation between features better. However, extracting the descriptive characteristics of medical images requires a certain prior knowledge, which is a challenging task. Therefore, this paper chooses to fuse MRI images and clinical indicators at the vector level.

A common vector-level fusion method aim is to connect two feature vectors end-to-end to generate a new feature vector. This method does not consider the relationship between two feature vectors. Canonical correlation analysis (CCA) is used in this chapter to analyze the correlation between image and index feature vectors, which will generate new fusion feature vectors. CCA is a statistical method for dealing with the interdependence between two random vectors. CCA plays a very important role in multi-source statistical analysis and also a valuable multi-source data processing method [18]. It is not only suitable for information fusion, but also suitable for removing redundant information.

In Fig. 6, assume that the MRI image feature vector is x and the clinical indicator feature vector is y . To extract typical related features, it is recorded as $\alpha^T x$ and $\beta^T y$ (one pair of typical variables), where $\alpha = (a_1, a_2, a_3, \dots, a_d)$ and $\beta = (b_1, b_2, b_3, \dots, b_d)$. The projection directions α and β can be obtained by maximizing the following criterion functions:

$$\rho = \frac{E[\alpha^T x y^T \beta]}{\sqrt{E[\alpha^T x x^T \alpha] E[\beta^T y y^T \beta]}} = \frac{\alpha^T E[xy^T] \beta}{\sqrt{\alpha^T E[xx^T] \alpha \times \beta^T E[yy^T] \beta}} = \frac{\alpha^T S_{xy} \beta}{\sqrt{\alpha^T S_{xx} \alpha \times \beta^T S_{yy} \beta}} \quad (9)$$

where S_{xx} and S_{yy} is covariance matrix, S_{xy} is the covariance matrix between x and y . The fusion feature vector can be obtained by multiplying the image feature vector and the

indicator feature vector with their corresponding typical variable α and β , as defined as follows:

$$C = (\alpha, \beta)^T (x, y) \quad (10)$$

where C is the fusion feature vector of image and indicator.

D. Disease classification diagnosis

This paper diagnoses Alzheimer's disease in three stages: control normal (CN), mild cognitive impairment (MCI) and Alzheimer's disease (AD), by inputting fusion feature vectors of images and indicators into the classifiers.

The multi-classifier selected in this paper is decision tree. Each internal node represents a test on an attribute, each branch represents a test output, and each leaf node represents a disease type. It represents a mapping relationship between object attributes and object values, using algorithms ID3, C4.5 and C5.0 spanning tree algorithm to use informatics theory of entropy.

IV. EXPERIMENT

The experimental dataset used in this study was obtained from Alzheimer's Disease Neuroimaging Initiative (ADNI). The dataset contains MRI images and clinical indicators. There are 302 patients in 3 categories: 91 in control normal (CN), 141 in mild cognitive impairment (MCI), and 70 in Alzheimer's disease (AD).

The MRI image uses three orthogonal planes section images obtained by T1 weighted and three-dimensional magnetization preparatory gradient echo sequences. It has high spatial and time resolution, high signal-to-noise ratio, small artifacts, and good contrast to the internal structure of the brain which is conducive to showing small brain changes.

There are 11 clinical indicators which come from demographic information, neuropsychological assessment and biological detection. The demographic information has two indicators: gender and age. Table 1 shows that there is no significant difference in the distribution of age, regardless of gender, in the three stages of AD.

Neuropsychological assessment consists of four scales: MMSE, CDR, RAVLT, and FAQ. Table 2 shows the Neuropsychological statistical assessment of patients with CN, MCI, and AD. The MMSE scores of patients from CN to AD decreased significantly, while the values of CDR, RAVLT and FAQ increased.

Biological detection consists of two amyloid proteins, two Tau proteins and apolipoprotein E. The changes of biomarkers were shown in Fig. 7. The levels of ABETA40 and ABETA42 in CN patients were lower than AD patients, APOE volume, and the levels of tau and P-tau were higher.

The proposed algorithm is validated in terms of accuracy. The accuracy is calculated as:

$$\text{Accuracy} = T \div C \times 100\% \quad (11)$$

where T is the correct number of samples and C is the total number of samples participating in the classification. The accuracy of the experiment results is obtained by calculating the average value of the five experiments.

TABLE I. DEMOGRAPHIC INFORMATION STATISTICS

	Gender	Age
CN	Male = 49	75.7±5.0 [65.8-85.5]
	Female = 42	
MCI	Male = 95	74.1±7.6 [59.2-89.1]
	Female = 46	
AD	Male = 37	74.7±7.8 [59.2-90.2]
	Male = 33	

Note: Gender Unit - Subjects, Age Unit - Year (Quantile Statistics of T Distribution)

TABLE II. NEUROPSYCHOLOGICAL ASSESSMENT STATISTICS

	MMSE	CDR	RAVLT	FAQ
CN	29.1±7.6 [27.1-31.1]	0.02±0.10 [-0.18-0.23]	3.35±3.0 [-2.60-9.30]	0.20±0.73 [-1.25-1.65]
MCI	27.1±1.8 [23.5-30.6]	1.61±0.93 [-0.23-3.45]	4.92±2.2 [0.54-9.30]	6.32±3.1 [-1.21-14.1]
AD	23.7±1.9 [19.8-27.5]	4.16±1.47 [1.24-7.09]	4.49±2.2 [0.46-8.51]	12.5±6.7 [-1.05-26.0]

Note: Scale Unit - Score (Quantile Statistics of T Distribution)

TABLE III. COMPARISON AMONG MULTI-CLASSIFICATION PERFORMANCE USING FOUR DIFFERENT BRAIN PLANAR IMAGES DATA

Data	Method	Accuracy
AXIALS-MRI	XY-CNN	48.3%
SAGITTAL-MRI	XZ-CNN	58.3%
CORONAL-MRI	YZ-CNN	51.7%
TOP-MRI	TOP-CNN-NN	75.0%

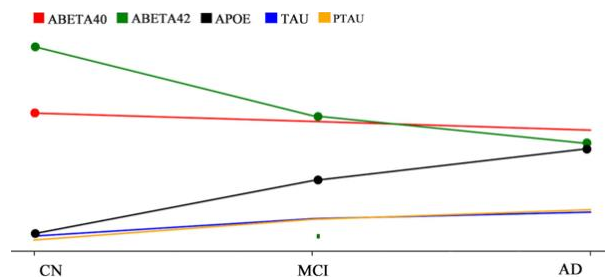
TABLE IV. COMPARISON BETWEEN THE PERFORMANCES OF MULTI-CLASSIFICATION MODELS BASED ON MEDICAL IMAGES

Author	Data	Method	Accuracy
TONG T [12]	MRI	NGF	56.3%
	MRI + PET	NGF	56.5%
LIU M [19]	MRI + PET	ISML	53.8%
Our Method	MRI	TOP-CNN-NN	75.0%
ZHE X [20]	MRI	SVM-RFE	85.6%

A. Evaluation of image feature extraction module

In this module, a TOP-CNN-NN model is constructed to extract the feature vector of MRI images. Table 3 shows the comparison among multi-classification performance based on different brain planar MRI images. The results show that the classification performance based on TOP-MRI images is better than that based on single plane MRI images. The experimental results verify the rationality of using three orthogonal planes MRI images in feature extraction module.

Table 4 shows performance comparison among multi-classification models based on medical images proposed by other papers and this paper. The experimental results show that the performance of this model is better than Tong T's NGF method [12] and Liu M's ISML method [19]. Although the performance of the model established in this paper is not better than the method based proposed by Zhe X [20], this proposed model does not need prior knowledge and clinicians' participation in the process of modeling.



Note: values of each index in the figure have been normalized, and the difference in vertical coordinates has no practical reference value. It mainly refers to the change of a single index.

Fig. 7. Breakdown Chart of Biological Detection Indicators Change

TABLE V. COMPARISON AMONG THE MULTI-CLASSIFICATION OF PERFORMANCE USING DIFFERENT TYPES OF CLINICAL INDICATOR

Data	Method	Accuracy
DEMOGRAPHIC-2	D-TREE	38.3%
	KNN	31.7%
NEUROPSYCHOLOGY-4	D-TREE	83.3%
	KNN	81.7%
BIOLOGY-5	D-TREE	43.3%
	KNN	45.0%
MERGE-28	D-TREE	78.3%
	KNN	75.0%
MERGE-11	D-TREE	85.0%
	KNN	78.3%

TABLE VI. MULTI-CLASSIFICATION PERFORMANCE COMPARISON WITH DIFFERENT COMBINATIONS OF IMAGES AND INDICATORS

Data	Accuracy
TOP-MRI	75.0%
CLINICAL	84.4%
MRI + CLINICAL	76.2%
TOP-MRI + CLINICAL + CCA	86.7%

B. Evaluation of indicator feature selection module

In this module, we use the CfsSubsetEval evaluator to evaluate the classification capabilities and the redundancy of each clinical indicator. This selected indicator is needed to compose clinical feature vector.

Table 5 shows the comparison among multi-classification performance of model using different types of clinical indicators. The data of 11 indicators includes 3 types (demographic, neuropsychology, biology). Performance of classification by only using neuropsychological assessment has almost similar performance compared to 11 merged indicators and slightly better in KNN method. However, using neuropsychological assessment alone is subjective.

C. Evaluation of feature vector fusion module

In this module, image feature vector and clinical feature vector are fused by using linear fusion method of multi-source data based on canonical correlation analysis (CCA). Table 6 shows the comparison of multi-classification performance among different combinations based on TOP-MRI images and clinical indicators. The experimental results show that performing linear fusion on TOP-MRI images and clinical indicators based on CCA gives the best performance.

TABLE VII. COMPARING MULTI-CLASSIFICATION PERFORMANCE OF VARIOUS MULTI-CLASSIFICATION DIAGNOSTIC ALGORITHMS

Author	Data	Method	Accuracy
TONG T [12]	MRI + CLINICAL	NGF	53.8%
ZHU X [21]	MRI + PET	SDFS	61.1%
ALTAFA T [11]	WHOLE MRI + CLINICAL	FF	75.0%
THIS PAPER	TOP-MRI + CLINICAL	OUR METHOD	86.7%

D. Evaluation of multi-classification algorithm

Table 7 shows the performance comparison between multi-classification diagnosis model proposed by other papers and multi-classification diagnosis model of fused images and indicators proposed in this paper. The accuracy of Tong T proposed graph-based non-linear fusion method (NGF) using CSF and genotype fusion of MRI, PET and clinical data was 53.8% [12]. The accuracy of Zhu X proposed method of sparse discriminant feature selection (SDFS) using MRI and PET images as experimental data was 61.1% [21]. In Altaf T proposed method by fusing the features of MRI images and other clinical data (FF) [11], the classification accuracy of fusion of whole brain images and clinical data was 75%. Compared with the multi-classification diagnosis model of Alzheimer's disease proposed in other papers, the accuracy of the model proposed in this paper can reach 86.7%. The experimental results verify that the multi-classification diagnosis model of Alzheimer's disease proposed in this paper is effective.

V. CONCLUSION

In this paper, we have presented a new multi-classification algorithm using linear fusion with TOP-MRI images and clinical indicators to diagnose AD. Experiments show that our method has high accuracy and effective in performing multi-classification diagnosis for AD.

Influence of extraction position of three orthogonal planes on classification performance can be explored more in the future. The sensitivity and specificity of indicators for differentiating types of diseases and improving the classification accuracy of AD can also be studied.

ACKNOWLEDGEMENT

This work was supported by the Special Fund of Shanghai Municipal Commission of Economy and Informatization (2017-RGZN-01004, XX-XXFZ-02-18-2666, XX-XXFZ-01-18-2604) and the National Key R&D Program of China under Grant 2019YFE0190500.

REFERENCES

[1] Wang Yutong, Xuan Zhidong. Progress in Epidemiology of Alzheimer [J]. Chinese Journal of Practical Neurological Diseases, 2015, 18(20):118-119.
 [2] Brookmeyer R, Johnson E Ziegler-Graham K et al. Forecasting the global burden of Alzheimer's disease[J]. Alzheimer's and Dementia, 2007, 3(3):186-191
 [3] Dallas P S, Cara L R, Naveed S A review of epidemiological evidence for general anesthesia as a risk factor for Alzheimer's

disease[J]. Progress in Neuro -Psychopharmacology & Biological Psychiatry, 2013(47):122-127
 [4] Wee C Y, Yap P T, Zhang D, et al. Identification of MCI individuals using structural and functional connectivity networks[J]. Neuroimage, 2012, 59(3):2045-2056.
 [5] S. Wang, Y. Zhang, G. Liu, P. Phillips, T.-F. Yuan, Detection of Alzheimer's disease by three-dimensional displacement field estimation in structural magnetic resonance imaging, J. Alzheimer's Dis. 50 (1) (2016) 233–248.
 [6] T. Altaf, S.M. Anwar, N. Gul, N. Majeed, M. Majid, Multi-class Alzheimer disease classification using hybrid features, Future Technologies Conference, IEEE (2017) 264–267.
 [7] Sarwinda D, Bustamam A. 3D-HOG Features -Based Classification using MRI Images to Early Diagnosis of Alzheimer's Disease[C]// 2018 IEEE/ACIS 17th International Conference on Computer and Information Science (ICIS). IEEE Computer Society, 2018.
 [8] Yuanyuan Chen, Haozhe Jia, Zhaowei Huang, Yong Xia: Early Identification of Alzheimer's Disease Using an Ensemble of 3D Convolutional Neural Networks and Magnetic Resonance Imaging. BICS 2018: 303-311
 [9] Karasawa H, Liu C L, Ohwada H. Deep 3D Convolutional Neural Network Architectures for Alzheimer's Disease Diagnosis[J]. 2018.
 [10] Platero C, Tobar M C. Combining a Patch-based Approach with a Non-rigid Registration-based Label Fusion Method for the Hippocampal Segmentation in Alzheimer's Disease[J]. Neuroinformatics, 2017, 15(2):165-183.
 [11] Altaf T, Anwar S M, Gul N, et al. Multi-class Alzheimer's disease classification using image and clinical features[J]. Biomedical Signal Processing and Control, 2018, 43:64-74.
 [12] Tong T, Gray K, Gao Q, et al. Multi-Modal Classification of Alzheimer's Disease Using Nonlinear Graph Fusion[J]. Pattern Recognition, 2016, 63:171-181.
 [13] Gu, J., Wang, Z., Kuen, J., Ma, L., Shahroudy, A., Shuai, B., Liu, T., Wang, X., Wang, L., Wang, G. and Cai, J., 2015. Recent advances in convolutional neural networks. arXiv preprint arXiv:1512.07108.
 [14] Chen Yi, Zhang Baorong. Advances in core biomarkers related to Alzheimer's disease [J]. life sciences, 2014, 26(01):2-8.
 [15] Johannes, Schröder, Elmar, Kaiser, Peter, Schönknecht, Aoife, Hunt, Philipp A, Thomann, Johannes, Pantel, Johannes, Schröder. [CSF levels of total tau protein in patients with mild cognitive impairment and Alzheimer's disease]. [J]. Zeitschrift für Gerontologie und Geriatrie, 2008, 41(6):497-501.
 [16] Hsiung G Y R, Sadovnick A D, Feldman H. Apolipoprotein E epsilon4 genotype as a risk factor for cognitive decline and dementia: data from the Canadian Study of Health and Aging [J]. Cmaj, 2004, 171(8):863-867.
 [17] Glenner GG, Wong CW. Alzheimer's disease: initial report of the purification and characterization of a novel cerebrovascular amyloid protein [J]. Biochemical and Biophysical Research Communications, 1984, 120(3):885-890.
 [18] Sun Quansen, Zeng Sheng-gen, Wang Ping-an, et al. Canonical correlation analysis theory and its application in feature fusion [J]. Journal of Computer Science, 2005, 28(9).
 [19] Liu M, Zhang D, Adeli E, et al. Inherent Structure-Based Multiview Learning with Multitemplate Feature Representation for Alzheimer's Disease Diagnosis[J]. IEEE Transactions on Biomedical Engineering, 2016, 63(7):1473-1482.
 [20] Zhe X, Yi D, Tian L, et al. Brain MR Image Classification for Alzheimer's Disease Diagnosis Based on Multifeature Fusion[J]. Computational and Mathematical Methods in Medicine, 2017, 2017:1-13.
 [21] Zhu X, Suk H I, Shen D. Sparse Discriminative Feature Selection for Multi-class Alzheimer's Disease Classification[M] Machine Learning in Medical Imaging. 2014.